BBA - Bioenergetics 1865 (2024) 149017

Contents lists available at ScienceDirect

BBA - Bioenergetics

journal homepage: www.elsevier.com/locate/bbabio

The cyanobacterial FtsH4 protease controls accumulation of protein factors involved in the biogenesis of photosystem I

Peter Koník [a,b], Petra Skotnicová [a], Sadanand Gupta [a,b], Martin Tichý [a], Surbhi Sharma [a,b], Josef Komenda [a], Roman Sobotka [a,b], Vendula Krynická [a,*]

[a] Institute of Microbiology of the Czech Academy of Sciences, Centre Algatech, Třeboň 379 01, Czech Republic
[b] Faculty of Science, University of South Bohemia, České Budějovice 370 05, Czech Republic

ARTICLE INFO

Keywords:
FtsH4 protease
Synechocystis
Photosystem I
Thylakoid membrane
Assembly factors

ABSTRACT

Membrane-bound FtsH proteases are universally present in prokaryotes and in mitochondria and chloroplasts of eukaryotic cells. These metalloproteases are often critical for viability and play both protease and chaperone roles to maintain cellular homeostasis. In contrast to most bacteria bearing a single *ftsH* gene, cyanobacteria typically possess four FtsH proteases (FtsH1–4) forming heteromeric (FtsH1/3 and FtsH2/3) and homomeric (FtsH4) complexes. The functions and substrate repertoire of each complex are however poorly understood. To identify substrates of the FtsH4 protease complex we established a trapping assay in the cyanobacterium *Synechocystis* PCC 6803 utilizing a proteolytically inactivated ^{trap}FtsH4-His. Around 40 proteins were specifically enriched in ^{trap}FtsH4 pulldown when compared with the active FtsH4. As the list of putative FtsH4 substrates contained Ycf4 and Ycf37 assembly factors of Photosystem I (PSI), its core PsaB subunit and the IsiA chlorophyll-binding protein that associates with PSI during iron stress, we focused on these PSI-related proteins. Therefore, we analysed their degradation by FtsH4 *in vivo* in *Synechocystis* mutants and *in vitro* using purified substrates. The data confirmed that FtsH4 degrades Ycf4, Ycf37, IsiA, and also the individual PsaA and PsaB subunits in the unassembled state but not when assembled within the PSI complexes. A possible role of FtsH4 in the PSI life-cycle is discussed.

1. Introduction

FtsHs are transmembrane metalloproteases universally conserved in bacteria, chloroplasts, and mitochondria. By modulating protein processing and turnover, the activity of FtsH proteases is essential for a broad spectrum of biological processes. In most bacteria, these enzymes are so crucial for maintaining cellular homeostasis that cannot be eliminated [1]. In cyanobacteria, algae and plants, FtsHs play an additional important role in the biogenesis of photosynthetic apparatus and the best-studied process involving FtsH in phototrophs is the quality control of the photosystem II complex (PSII) (reviewed in [2]). However, the contribution of FtsHs to photosystem I (PSI) biogenesis [3] and to plastid development [4] has also been proposed.

The molecular mechanisms, by which FtsHs control the biogenesis of photosynthetic complexes remain mostly unknown and only a few substrates of FtsHs related to photosystem biogenesis were identified in phototrophs [5–7]. Likewise the other cyanobacteria, the model species *Synechocystis* sp. PCC 6803 (hereafter *Synechocystis*) contains four FtsH homologues, FtsH1-FtsH4. Individual *Synechocystis* FtsHs form three oligomeric complexes *in vivo* — two heteromers FtsH1/3 and FtsH2/3, and homomeric FtsH4. The FtsH2/3 and FtsH4 complexes have been localized in the thylakoid membrane (TM) and levels of these complexes are comparable [7,8]. Similarly to its *Arabidopsis thaliana* orthologs FtsH2/8 and FtsH1/5 [9], the *Synechocystis* FtsH2/3 complex plays a pivotal role in the selective degradation of PSII subunits during PSII repair [10,11] and controlling the level of unassembled PSII subunits [12]. The deletion of *ftsH2* gene causes light sensitivity and photoinhibition of PSII [10]. Nonetheless, the role of FtsH2/3 is clearly not restricted to maintaining active PSII complexes. The inactivation of FtsH2 protease leads to other phenotypic changes such as a reduced level of PSI and a significant decrease in the cellular level of chlorophyll (Chl) [13].

The less abundant, but essential FtsH1/3 complex is located in the plasma membrane [14,15] and is more specifically involved in the

* Corresponding author at: Institute of Microbiology of the Czech Academy of Sciences, Centre Algatech, Třeboň 379 01, Czech Republic.
E-mail address: krynicka@alga.cz (V. Krynická).

https://doi.org/10.1016/j.bbabio.2023.149017
Received 30 May 2023; Received in revised form 18 September 2023; Accepted 4 October 2023
Available online 11 October 2023
0005-2728/© 2023 Elsevier B.V. All rights reserved.

acclimation of cells to nutrient deficiency. Several transcription factors, regulating mostly nutrient starvation genes, have been identified as potential substrates of FtsH1/3 [16]. In contrast to the essential role of FtsH1 and FtsH3 and poor viability of the FtsH2-less strain, the elimination of FtsH4 had no obvious negative impact on the *Synechocystis* growth under normal growth conditions (40 μmol of photons m^{-2} s^{-1}, 28 °C [13]) apart from a statistically significant higher level of Chl per cell compared with wild type (WT) [7]. This excess of Chl was incorporated into the PSI trimer (PSI [3]), the level of which was elevated in Δ*ftsH4* cells compared with WT [7].

This subtle phenotype of the *Synechocystis* Δ*ftsH4* strain, observed under moderate light intensities, contrasts to strongly retarded growth of this mutant under high light (HL) [7]. Interestingly, even more severe growth defects have been described for the Δ*ftsH4* mutant cells that were first grown to stationary phase and then diluted and shifted to HL [7]. Our recent results exclude that the *Synechocystis* FtsH4 structurally or functionally substitutes for FtsH2 and hence the FtsH2/3 complex in the repair of PSII. Instead, the FtsH4 acts in the photoprotection of PSII by dual regulation of high light-inducible proteins (Hlips). These small, single-helix proteins bind Chl and carotenoids and are crucial for the biogenesis of PSII under stress conditions [17,18]. FtsH4 positively regulates the expression of *hli* genes coding for Hlips, shortly after HL exposure but is also responsible for the post-stress removal of Hlips once they are no longer needed. In *Synechocystis*, FtsH4 complexes are concentrated in well-defined membrane regions at the inner and outer periphery of the thylakoid system. As the FtsH4 has been co-purified with a similar set of protein factors as the PSII assembly intermediates [19], it is likely that the observed FtsH4-rich membrane spots co-localize with compartments where the biogenesis of photosystems takes place.

In this work, we screened for substrates of the *Synechocystis* FtsH4 using a proteolytically inactive FtsH4 variant as a trap. Putative substrate proteins, co-isolated with inactive protease, were verified *in vivo* by employing *Synechocystis* FtsH4 mutants and *in vitro* using a proteolytic essay. We can conclude that the FtsH4 controls the level of at least two PSI assembly factors (Ycf37 and Ycf4), the unassembled PSI core subunits and the PSI-binding IsiA protein. Other potential substrates are also discussed.

2. Material and methods

2.1. Construction of Synechocystis strains

The *Synechocystis* glucose tolerant substrain GT-P [20] was used as WT for all experiments described in this study. The Δ*ftsH4* mutant and *Synechocystis* strains expressing C-terminally 3xFLAG-tagged FtsH4 under *psbA2* promoter (F4CF strain) and C-terminally 6xHis-tagged FtsH4 (*ftsH4-his*) under the native *ftsH4* promoter are described in [7]. To construct the ^{trap}*ftsH4-his* strain, the E439Q mutation was introduced into the *ftsH4-his* plasmid [7] using the QuikChange II XL site-directed mutagenesis kit (Agilent Technologies). The resulting plasmid was transformed into *Synechocystis* and transformants were fully segregated using an increasing concentration of chloramphenicol. The presence of ^{trap}*ftsH4-his* gene was confirmed by sequencing. The A3 strain, lacking *psbAI* and *psbAII* genes [21] was used as a control for the F4CF strain.

To construct *Synechocystis* strains expressing N-terminally 1xFLAG-tagged PsaA (f.PsaA) or PsaB (f.PsaB) from the native *psaAB* promoter, a set of DNA constructs was prepared by the NEBuilder HiFI DNA assembly kit, each containing the gentamycin or chloramphenicol resistance cassette downstream of the *psaAB* locus (see Fig. S1). These constructs were used to replace the whole *psaAB* operon to obtain strains expressing only f.PsaA or f.PsaB (*f.psaA*/Δ*psaB* or *f.psaB*/Δ*psaA* strains). The *f.psaA* strain, containing the assembled FLAG-PSI with tagged PsaA, was prepared by transforming the *f.psaA*/Δ*psaB* strain using the *psaB*-Gent construct and selecting for autotrophy (Fig. S1).

2.2. Cultivation of Synechocystis strains

Liquid cultures were grown in BG-11 medium in Erlenmeyer flasks at 28 °C on a rotary shaker (120 rpm) at a normal irradiance of 40 μmol photons m^{-2} s^{-1} (normal light, NL) or a high irradiance of 500 μmol photons m^{-2} s^{-1} (HL) provided by white fluorescence tubes. For FtsH4-His pulldown assays, *Synechocystis* strains were grown in 1 L cylinders bubbled with air at irradiance of 100 μmol photons m^{-2} s^{-1} which was increased to 300 μmol photons m^{-2} s^{-1} for 16 h before harvesting. PSI strains for FLAG-specific pulldowns were cultivated in a 10 L flask (culture volume 4 L) bubbled with air at 5 μmol photons m^{-2} s^{-1}.

For the cold stress experiment, strains were cultivated at 20 °C at irradiance of 150 μmol photons m^{-2} s^{-1}.

To inhibit the protein synthesis, the liquid cultures were supplemented with lincomycin at a concentration of 100 μg ml^{-1} of culture.

To remove iron, the cells were transferred to an iron-depleted medium (residual concentration of iron about 5 μM) supplemented with 10 μM deferoxamine B (DFB), an iron chelator. Cells were cultivated for another 72 h. For recovery from iron depletion, the cells were washed three times, resuspended in standard BG11 and grown for another 48 h.

2.3. Whole cell absorption spectroscopy and Chl determination

Absorption spectra of whole cells resuspended to the same OD_{750nm}, were acquired at room temperature using a UV-3000 spectrophotometer (Shimadzu, Japan). For routine Chl determination, methanol extracts of cell pellets or membranes were analysed spectroscopically according to Porra et al. [22].

2.4. Low temperature fluorescence spectroscopy

Low temperature Chl fluorescence emission spectra were measured at 77 K in cultures with the identical OD_{750nm} using an SM 9000 spectrophotometer (Photon Systems Instruments, Czech Republic) at an excitation wavelength of 470 nm.

2.5. Isolation of thylakoid membranes

Approximately 100 ml of cells at an OD_{750nm} of ~0.8 were harvested by centrifugation at 6000 ×*g* for 10 min and resuspended in buffer A (25 mM MES, pH 6.5, 10 mM $CaCl_2$, 10 mM $MgCl_2$, 25 % glycerol) for protein analysis and FLAG-tag specific pulldowns or buffer B (25 mM Na phosphate buffer, pH 8, 50 mM NaCl, 10 % glycerol) for His-tag specific pulldowns. Cells were mixed with 100–200 μm diameter glass beads in 1:1 ratio (1 volume of dense cell solution with 1 volume of glass beads) and broken (6 × 20 s) using a mini-bead beater. To separate soluble and membrane fractions, samples were centrifuged at 30,000 ×*g* for 20 min at 4 °C. Pelleted membranes were washed once with an excess of buffer and then resuspended in 150 μl of buffer A or B for later use.

2.6. Electrophoresis and immunoblotting

For 1D SDS-PAGE, membrane proteins were denatured with 2 % SDS (w/v) and 1 % (w/v) dithiothreitol for 30 min at room temperature and analysed by SDS-PAGE in a denaturing 12–20 % polyacrylamide gel containing 7 M urea or in 4–15 % TGX precast gels (Bio-Rad). For the clear native (CN) electrophoresis, the proteins were separated on 4–14 % (w/v) polyacrylamide gel as described in Komenda et al. [23] or 4–15 % TGX precast gel (Bio-Rad). The protein gels were scanned and the Chl fluorescence image was taken by LAS-4000 camera (Fuji). Individual components of protein complexes were resolved by incubating the gel strip from the first dimension in 2 % (w/v) SDS and 1 % (w/v) dithiothreitol for 30 min at room temperature and then proteins were separated in the second dimension by a 12–20 % linear gradient SDS-PAGE gel containing 7 M urea. Proteins in gels were stained by SYPRO Orange (Sigma-Aldrich) or Coomassie Blue (Bio-Rad).

For immunodetection, proteins were transferred from the SDS gel to a polyvinylidene difluoride (PVDF) membrane (Immobilon-P, Merck Millipore). Membrane was incubated with the primary antibody and subsequently with an anti-rabbit secondary antibody conjugated with horseradish peroxidase (Sigma-Aldrich). Chemiluminescence obtained using an Immobilon Crescendo substrate (Millipore) was imaged using the LAS-4000 camera (Fuji). These primary antibodies, specific for the following proteins and tags, were used in this study: FtsH4 [24], PsaA (Agrisera, cat. no. AS06 172), PsaB (Agrisera, cat. no. AS10 695), PsaD [25], Ycf4 (Agrisera, cat. no. AS07274), Ycf37 [26], 6xHis (Abcam, cat. no. ab9108), and FLAG (Abgent, cat. no. AP1013A).

2.7. Pulldown of tagged proteins

For the purification of His-tagged FtsH4 variants, 3.5 L of *Synechocystis* cells were broken using glass beads as described above in buffer B with EDTA-free protease inhibitor (Sigma). The pelleted membrane fraction, prepared essentially as described in Koskela et al. [27], was resuspended in buffer B (~0.5 mg Chl/ml) and solubilized for 60 min at 10 °C with 1 % 4-trans-propylcyclohexyl α-maltoside. Finally, insoluble contaminants were removed by centrifugation (47,000 ×*g*, 20 min). Pulldown was performed as described in Krynická et al. [7]; F.PsaA and F.PsaB were purified in buffer A as described in Koskela et al. [27].

2.8. FtsH in vitro assay

Proteolytically active FtsH4-His was isolated from *Synechocystis* membrane fraction as described above. The FtsH protease assay was carried out essentially according to Tomoyasu et al. [28] and Krynická et al. [7] using 0.3 μg of total FtsH4 and 0.2 μg of the substrate. For the inhibition of FtsH activity, the reaction was supplemented with cOmplete Protease Inhibitor Cocktail (Roche) containing EDTA. The reaction was carried out in 20 μl. Composition of the reaction buffer: 25 mM MES pH 6.5, 5 % glycerol, 2 mM Mg^{2+}, 2 mM Ca^{2+}, 0.4 μM Zn^{2+}, 3 mM ATP, and 0.04 % 4-trans-propylcyclohexyl α-maltoside. All samples were incubated for 3 h at 37 °C. After incubation, the samples were denatured by 1 % SDS, separated by 1D SDS-PAGE, and the presence of F.PsaA, F.PsaB, Ycf37, and FtsH4 was detected by specific antibodies, protoporphyrinogen IX oxidase (HemJ) was detected by FLAG-specific antibody. Quantification of the detected bands was performed by AzureSpot Pro software v. 2.2.167 (Azure Biosystems). The substrate amount is expressed as a percentage of the initial substrate level (100 %) and numbers represent means of 3 independent reactions ± standard deviation.

2.9. Analysis of His-tagged FtsH4 pulldowns by protein MS

For the eluates of His-tagged proteins, 5 μl were diluted in 45 μl of 0.1 % (v/v) Rapigest (Waters) surfactant in 50 mM ammonium bicarbonate. The final mixture was incubated for 45 min at 60 °C, cooled briefly and proteomic grade trypsin (Sigma) was added to a final concentration of 10 ng/μl and incubated at 37 °C. After 12 h, samples were acidified by adding formic acid to a final concentration of 0.5 % (v/v). The sample was desalted and peptides were isolated by the StageTip procedure [29]. LC-MS/MS analysis was performed on an UltiMate 3000 UHPLC (Thermo Fisher Scientific) on-line coupled to a TimsTOF pro (Bruker) mass spectrometer. 2 μl of the sample were trapped for 1 min on a ThermoFisher trap (0.3 × 5 mm, C18, 5 μm) column, then separated by reverse phase liquid chromatography on an Acclaim PepMap RSLC column (75 μm × 15 cm, C18, 2 μm, 100 Å; Thermo Fisher Scientific) column. Peptides were eluted by a linear water: acetonitrile gradient, where acetonitrile increased from 3 to 50 % over 30 min and the eluted fluid was fed directly into the CaptiveSpray nano ion source of the mass spectrometer. Both mobile phases contained 0.1 % of formic acid. Spectra were acquired in a data-dependent PASEF (Parallel Accumulation/SErial Fragmentation) regime with an accuracy of 0.2 ppm for precursors and 0.5 ppm for fragments. 3 technical replicates were acquired for each of the 3 biological replicates for each sample. Raw data were processed by the MaxQuant/Andromeda software [30,31] and matched to species-specific *Synechocystis* protein databases downloaded from Uniprot and Cyanobase. Statistical analysis of protein groups obtained from MaxQuant was performed in Perseus 1.6.14.0 [32]. After removing hits identified only by modified peptides, reverse database hits and most common contaminants, IBAQ intensities were log_2-transformed and missing data was imputed from normal distribution. Interactors were identified by comparing FtsH4-His with ^{trap}FtsH4-His samples using the volcano plot function, and non-specific reactions were identified by subtracting proteins identified in the non-his control sample. The MS proteomics data were deposited to the MassIVE, ID: MSV000092109.

3. Results

3.1. Pulldown assay using His-tagged FtsH4 as a bait

To establish a sensitive trap assay for the identification of FtsH4 substrates, we constructed *Synechocystis* strains expressing the active 6xHis-tagged FtsH4 variant and its proteolytically inactive derivative (^{trap}FtsH4-His) from the native *ftsH4* promoter. The inactive enzyme contains a point mutation E439Q abolishing the binding of the catalytic zinc ion [33]. The FtsH trap is still able to unfold and translocate substrates into the proteolytic chamber allowing to isolate stable FtsH-substrate complexes [34]. As confirmed by immunodetection, the levels of FtsH4-His and ^{trap}FtsH4-His were comparable with the level of native FtsH4 protease (Fig. S2). In order to find the optimal conditions for the purification of both active and inactive FtsH4 proteins we analysed the level of FtsH4 during different phases of growth. Notably, the highest accumulation of this protease was observed in the linear growth phase, followed by lag and stationary phase while the lowest level was found in the exponential growth phase (Fig. S3A).

To distinguish between potential FtsH4 substrates and proteins interacting in the cell with the FtsH4 enzyme for other reasons, we first performed a pulldown assay with the FtsH4-His as a control for ^{trap}FtsH-His. Both strains were cultivated in three independent parallels in 1 L cylinders under NL conditions till the linear growth phase (OD_{750nm} ~ 2.5) to ensure a high cellular accumulation of FtsH4 (see Fig. S3A, B). After cell disruption, FtsH4 protease was purified on a nickel column and subjected to nanoLC-MS/MS protein identification (Fig. 1). Raw data were processed using MaxQuant and the obtained IBAQ intensities were used to determine statistically enriched proteins [7,35]. Solubilized membrane proteins from WT were used as a negative control for the detection of non-specific interactors with the resin.

This analysis revealed 256 proteins that were significantly enriched compared to the WT TM control when the false discovery rate cut-off was 1 % (FDR = 0.01). Applying more stringent significance criteria: log2 FC (FtsH4 — WT) ≥ 3, which means 8 (2^3) times higher iBAQ intensity than the WT control (Fig. 1A, blue area), and corresponding to at least 1 % of the FtsH4 content, we selected the 51 hits (Fig. 1A, red square, Supplementary Dataset 1). The eight most abundant proteins (above 10 % of FtsH4 content) are listed in Table 1. Sll1106 protein is known to interact tightly with FtsH4 [7] and, indeed, Sll1106 was among the most abundant hits in our FtsH4 pulldown (36 % of the FtsH4 content). Apart from Sll1106, FtsH4 was co-isolated with GlgB and GlgA2 enzymes functioning in glycogen synthesis (75 % and 11 % of the FtsH4 iBAQ content) and Slr0374 protein (69 % of the FtsH4 content) that is involved in CO_2 uptake and utilization [36]. Glutamine synthetase was an additional enzyme among the most abundantly purified proteins with FtsH4 (47 % of the FtsH4 content). Finally, the set of top eight co-purified proteins comprised two transcriptional repressors including Fur that regulates gene expression in response to iron depletion (Table 1).

In agreement with our previous FLAG-FtsH4 pulldown (see

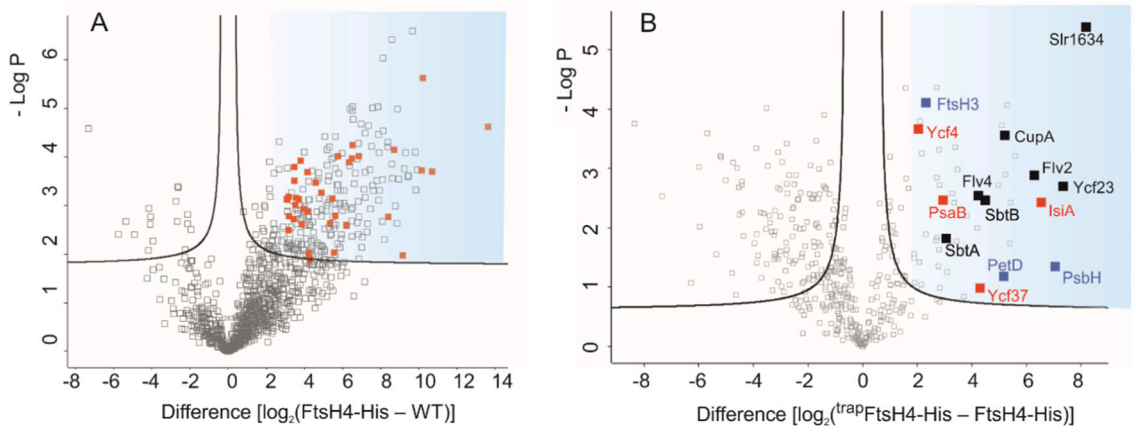

Fig. 1. Identification of candidate proteins for FtsH4-His substrates using ^{trap}FtsH4-His assay and protein MS. A) Volcano plot representing the difference in Log_2-transformed iBAQ intensities between FtsH4-His pulldown and the control WT TM elution. Three independent biological triplicates were carried out for both pulldowns; identified protein hits are indicated by grey squares. The FDR cut-off, represented by black line, was set to 1 % and proteins highlighted in red are the most significantly enriched with the highest abundance in comparison with the bait (Supplementary Dataset 1). B) Volcano plot representing the difference in Log_2-transformed iBAQ intensities between FtsH4-His and ^{trap}FtsH4-His pulldowns. Three independent biological triplicates were carried out for both pulldowns. Proteins (potential substrates) significantly enriched in the trap elution compared to FtsH4-His elution are inside the blue background rectangle. Proteins related to PSI are highlighted in red and proteins involved in CO_2 uptake are in black; other photosynthetic proteins are in blue. (For interpretation of the references to colour in this figure legend, the reader is referred to the web version of this article.)

Discussion section), we also identified CurT protein that is important for the organization of TM, RubA protein that is important for the PSII assembly [37], and several subunits of ATP synthase (Supplementary Dataset 1). However, all these proteins were represented only in units of percent relative to the FtsH4 iBAQ intensity and these are more likely only co-localized with FtsH4 or bind this protease transiently/very weakly.

After clarifying what proteins co-isolate with the active FtsH4-His, we purified the ^{trap}FtsH4-His protease and searched for specific hits that are absent or significantly less abundant in controls (FtsH4-His and WT TM). Using FDR = 0.05, we identified 64 proteins significantly enriched in trap pulldown (Fig. 1B). To narrow down the list of potential FtsH4 substrates, we defined more stringent criteria for significance: log_2 FC (^{trap}FtsH4-His – FtsH4-His) $\geq$ 2, which means 4 times more than in the FtsH4-His control. With this setting, 42 proteins were identified in total (Fig. 1B, blue area, Table S2). Most of these putative FtsH4 substrates were transmembrane and membrane-associated proteins and, quite specifically, proteins involved in photosynthesis.

Table 1
A list of proteins that were most abundantly represented in the His-tagged FtsH4 pulldown. Raw iBAQ intensities of proteins, co-eluted with FtsH4-His, were compared with their iBAQ intensities in the control elution. Log_2FC (FtsH4-His — WT) shows the Log_2 difference (enrichment) in the FtsH4-His sample compared to the control. The column labelled % of FtsH4 shows the calculated percentage of iBAQ intensities of the co-eluted proteins in respect to the bait protein (FtsH4-His). Only proteins with Log_2FC $\geq$ 3 and a percentage above 10 % are shown (see the Supplementary Dataset 1 for the full list of proteins). Experiments were performed in triplicates; averaged values are shown.

Number	Protein	iBAQ intensity FtsH4-His	WT	Log2FC (FtsH4-His − WT)	−log *P* value	% of FtsH4
	FtsH4 (Sll1463)	20,455,700	1908	14	5	100
1	GlgB (Sll0158)	13,336,700	1,229,830	3	4	75
2	Slr0374	11,833,400	146,968	6	4	69
3	GuaA (Slr0213)	8,556,310	1,043,050	3	2	47
4	Sll1106	6,887,130	99,608	6	4	36
5	Fur (Sll0567)	5,232,910	226,268	5	3	29
6	Slr1617	3,054,720	89,864	5	3	18
7	NrdR (Sll1780)	2,551,290	75,893	5	3	14
8	GlgA2	2,507,480	180,845	4	3	11

3.2. Identification of putative substrates using a protease trap assay

Interestingly, several proteins enriched in the ^{trap}FtsH4-His preparation were related to PSI and its biogenesis, namely IsiA, PsaB, Ycf4, and Ycf37. IsiA is the iron stress-induced Chl-binding protein that forms an oligomeric ring around the PSI under iron limitation [38,39]. PsaB is the core subunit of the PSI complex [40,41] and Ycf4 and Ycf37 are PSI assembly factors involved in the early stage of the PSI biogenesis [42,43]. PsaA was also enriched in the trap pulldown compared to active FtsH4, however since its level was relatively high in the WT control, the specific occurrence of PsaA in the pulldown was questionable. Notably, the amount of PsaA was 2.5 times lower than PsaB in the trap indicating that FtsH4 prefers PsaB to PsaA.

Apart from the PSI-related proteins, PsbH and PetD were also enriched in the ^{trap}FtsH4-His elution. PsbH is a small PSII subunit associated with the CP47 antenna protein and PetD (Slr0343) is a component of the cytochrome b_6f complex that mediates the electron transfer between PSII and PSI as well as the cyclic electron flow around PSI. In addition, we found prohibitin Phb1 and FtsH3 but not FtsH1 and FtsH2, as potential substrates of FtsH4. It is also worth noting that 8 of 44 selected proteins are involved in acclimation to low carbon and their expression increases during the CO_2 limitation, namely flavoproteins Sll0217, Sll0219, SbtA, SbtB, CupA and several proteins of unknown function like Ycf23 and Slr1634 [44]. However, as in the case of IsiA, our cell cultures were not stressed by CO_2 limitation, which is evident from low levels of bicarbonate or CO_2 transporters such as SbtA or CupA in the membrane fraction (Fig. S4). Finally, two heat shock proteins were found among the putative substrates of FtsH4.

3.3. FtsH4-less cells contain aberrant levels of PSI subunits and PSI assembly factors under stress conditions

The FtsH trap approach revealed two PSI assembly factors (Ycf37, Ycf4) and PsaB, the core subunit of the PSI complex, as putative substrates of FtsH4. Our previous study demonstrated that the deletion of *ftsH4* results in a surplus of PSI trimer under NL conditions (Fig. S5) [7].

Interestingly, after 5 days at 20 °C (cold-stress conditions), in the Δ*ftsH4* strain, we identified two additional PSI complexes migrating between the PSI monomer and the dimer in CN gel (Fig. 2A, blue and red arrow). These are presumably intermediates of PSI assembly since complexes of the same size were observed in 2D autoradiogram that is indicative of newly synthesized PsaA/PsaB proteins (Fig. 2B).

Since the presence of these PSI assembly intermediates could be related to the overaccumulation of Ycf37 and Ycf4 PSI assembly factors in Δ*ftsH4*, we tested it using the 2D blots of membranes from cells grown in cold-stress which were probed with antibodies specific for each assembly factor. Indeed, the content of Ycf37 was significantly increased in Δ*ftsH4* compared with WT (Fig. 2A) and a smearing signal of Ycf37 starting in the region of these complexes indicated their possible association with this assembly factor. We could not immunochemically detect Ycf4 on the 2D gel but it was possible on 1D gel and the analysis confirmed the overaccumulation of both, Ycf37 and Ycf4 in cold stress-treated Δ*ftsH4* cells (Fig. 2C). In contrast to cold stress, amounts of Ycf37 and Ycf4 were comparable in WT and Δ*ftsH4* under NL (Fig. 3A). Nonetheless, after the transfer of cells to HL conditions, effectively blocking the synthesis of PSI [45,46], the amount of Ycf4 and partly also Ycf37 assembly factor decreased in WT while it remained stable in Δ*ftsH4* after 72 h (Fig. 3A). 2D gel analysis of WT and Δ*ftsH4* cells after 24 h of HL supported these results (Fig. 3B) and a distinct band of Ycf37 in the region of the red-designated PSI complex of Δ*ftsH4* supports its identity as a PSI monomer with bound Ycf37. Notably, quite the opposite effect was observed in the F4CF strain overexpressing the FLAG-tagged FtsH4 [7]. The level of the Ycf37 protein was lower when compared with the control *psbAII* deletion strain A3 [21] after 24 h of HL (Fig. 3B).

As Ycf37 and Ycf4 accumulate in the mutant lacking FtsH4 and conversely, their levels are lower in the mutant overexpressing F4FC, these results strongly support the conclusion that these PSI assembly factors are substrates of FtsH4. To further confirm this hypothesis, we performed an FtsH4 *in vivo* degradation assay. In WT and Δ*ftsH4*, we monitored a decrease in Ycf37 and Ycf4, and for control also D1, after exposure to HL and inhibition of new protein synthesis by the addition of Lincomycin. While in WT we observed a reduction in the amount of all proteins during 6 h of HL exposure, in Δ*ftsH4* the amount of only D1 protein decreased comparably to WT while the amount of Ycf37 and Ycf4 did not decline (Fig. 3C).

3.4. *FtsH4 protease is involved in IsiA degradation during the recovery from iron depletion*

IsiA belonged to the most enriched proteins in the ^{trap}FtsH4-His pulldown (Fig. 1B, Table S2). Although the function of this protein is not completely clarified, IsiA has been proposed to serve as a Chl storage protein or an energy sink under stress conditions, most prominently

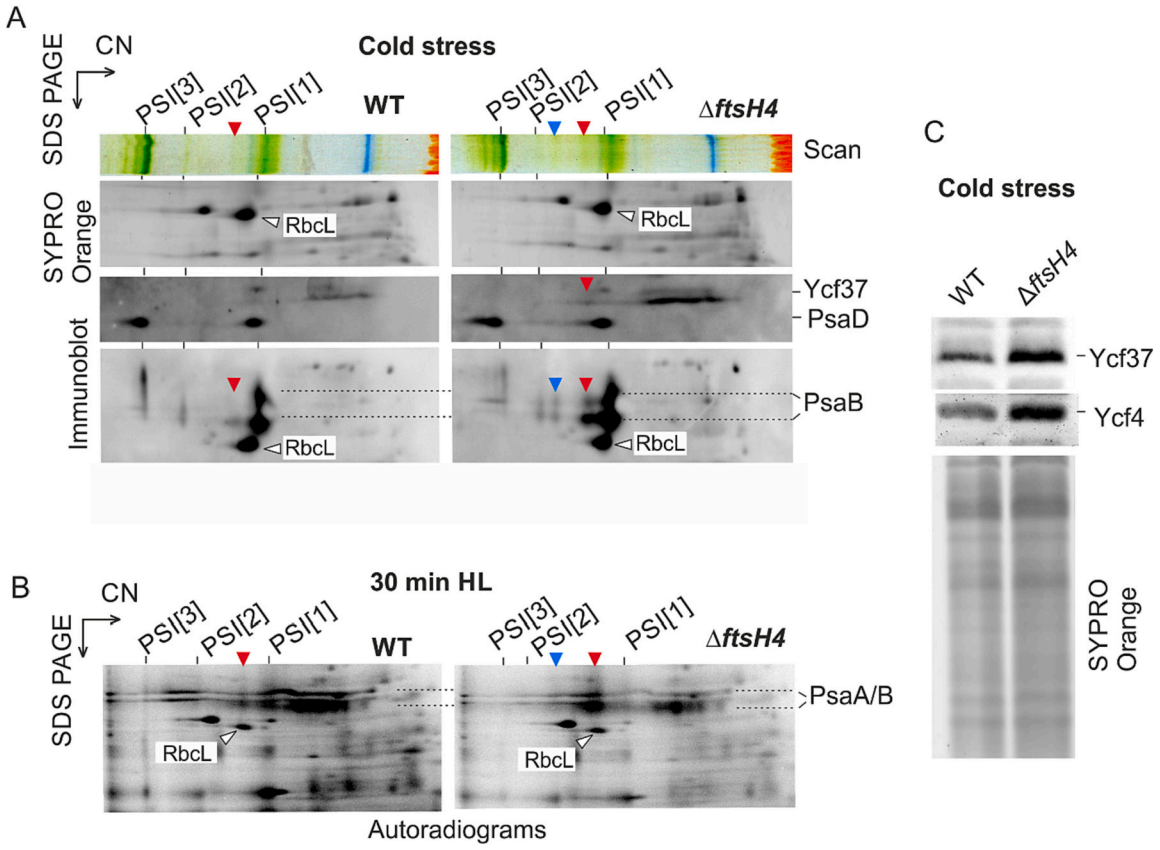

Fig. 2. Accumulation of PSI and PSI assembly complexes in the Δ*ftsH4* mutant grown in stress conditions. A) TM were isolated from WT and Δ*ftsH4* cells grown for 5 days under cold stress (20 °C/150 μmol of photons m^{-2} s^{-1}) and analysed by 2D CN/SDS-PAGE. The CN gel was scanned (Scan). The 2D SDS gels were stained by SYPRO Orange, electroblotted to PVDF membrane and the blot probed with antibodies specific for PsaB, Ycf37, and PsaD. PsaB migrates in the SDS gel in two forms differing in the degree of denaturation (marked with dash-line). The SYPRO Orange stained gels document equal loading. Designation of complexes: PSI[1], PSI[2], and PSI[3]: PSI monomer, dimer and trimer, respectively; and large subunit of RUBISCO (RbcL) is also indicated. Red and blue arrows in 2D blot indicate PSI assembly complexes; 2.5 μg of Chl of each sample was loaded on the 2D gel and 1 μg of Chl for the 1D SDS gel. B) The position of PSI assembly complexes indicated on immunoblot by red asterisks (A) were compared with 2D autoradiogram of membranes isolated from cells grown under standard conditions, radio-labelled and treated with HL (500 μmol of photons m^{-2} s^{-1}) for 30 min before the membrane isolation. The radio-labelled gels were exposed in a phosphoimager overnight. C) The same samples as in (A) were separated by SDS-PAGE, blotted and probed by antibodies against Ycf37 and Ycf4. (For interpretation of the references to colour in this figure legend, the reader is referred to the web version of this article.)

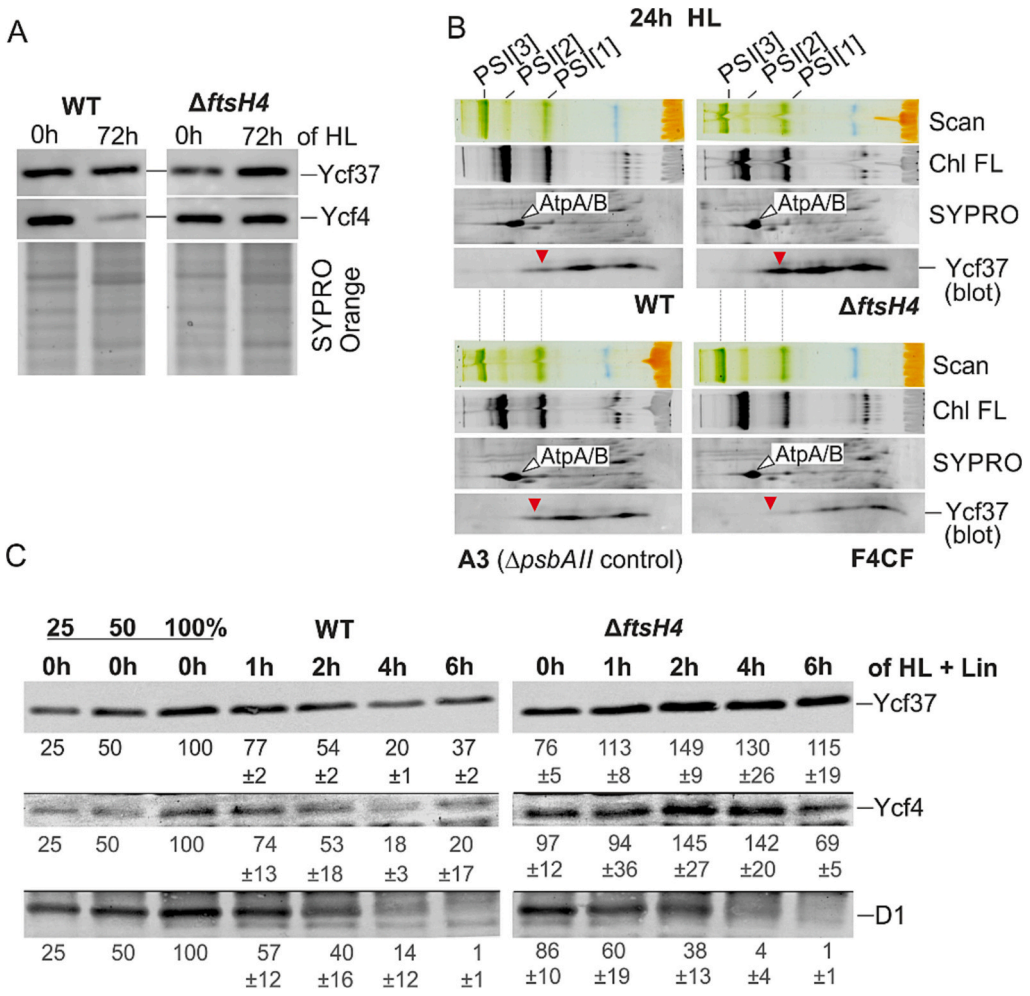

Fig. 3. Effects of the *ftsH4* deletion or overexpression on the amount of PSI assembly factors under HL conditions. A) SDS-PAGE analysis of TM isolated from WT and Δ*ftsH4* strains exposed to HL for 72 h (28 °C/500 μmol photons m^{-2} s^{-1}). The SDS gels were stained by SYPRO Orange, electroblotted to PVDF membrane and the blot probed with antibodies specific for Ycf37 and Ycf4. *Loaded samples were* normalized *per* number of cells. B) 2D CN/SDS-PAGE and immunoblot of TM proteins prepared from WT, Δ*ftsH4*, A3, and F4CF cells grown for 24 h under HL (28 °C/500 μmol photons m^{-2} s^{-1}). The CN gel was scanned (Scan) and Chl autofluorescence was detected (Chl FL); 2.5 μg of Chl was loaded per each sample. The SYPRO Orange stained gels are shown as a loading control. Designation of complexes: PSI[1], PSI[2] and PSI[3]: PSI monomer, dimer and trimer, respectively; AtpA/B: α/β subunits of ATP synthase. C) SDS-PAGE analysis of TM isolated from WT and Δ*ftsH4* strains supplemented with lincomycin and exposed to HL for 6 h. The SDS gels were electroblotted to PVDF membrane and the blot was probed with antibodies specific for Ycf37, Ycf4 and D1. *Loaded samples were* normalized *per* number of cells. The obtained protein signals were quantified by AzureSpot Pro software v. 2.2.107 (Azure Biosystems). A ratio (percentage) of each analysed substrate in comparison to 100 % in calibration is shown, values are means of 3 independent measurements ± standard deviation.

under iron depletion [39,47]. To test whether the IsiA is degraded by the FtsH4 protease *in vivo*, we monitored the level of IsiA in WT and Δ*ftsH4* cells during recovery from iron depletion. Initially, we exposed both strains to iron stress to induce the expression of *isiA* gene; iron-depleted conditions were induced by transferring the cells grown in BG11 to the BG11 lacking iron ($-Fe^{2+}$) and supplemented by Deferoxamine B chelator to remove iron traces.

After 72 h of the low-iron stress, we observed no difference in the level of IsiA in WT and Δ*ftsH4* strains (Fig. 4). However, when we replaced the medium with normal BG11 supplemented with iron, the degradation of IsiA in the mutant was clearly retarded. The difference was most prominent after 24 h of the recovery when the WT contained 40 % of the initial IsiA level while Δ*ftsH4* values remained twice as high (Fig. 4). Because FtsH4 was purified with Fur, which functions as a repressor of IsiA expression, we wanted to exclude the possibility that the accumulation of IsiA in ΔftsH4 is due to lower levels of Fur protein. Therefore, we also monitored the level of Fur during recovery from iron depletion. Nevertheless, in agreement with [15] the Fur levels increased during the course of recovery in both WT and ΔftsH4. Thus, we concluded that slower decrease in the IsiA level during recovery from iron depletion in the ΔftsH4 is not related to the lower accumulation of Fur and that the data support involvement of FtsH4 in the degradation of IsiA.

3.5. Validation of putative FtsH4 substrates using an in vitro FtsH assay

Results of the FtsH4 trap approach as well as the analysis of protein content in FtsH4 mutant strains indicated that PSI assembly factors, the PsaB PSI subunit and IsiA are potential substrates. To confirm that the FtsH4 can recognize and degrade these proteins, we performed an *in vitro* assay of FtsH4 proteolytic activity using the purified FtsH4-His as an active enzyme (see Material and Methods). For negative control, the protease activity was inhibited with EDTA. We tested first purified FLAG-PSI complexes, isolated from the strain expressing FLAG-tagged *psaA* instead of *psaA* (*f.psaA* strain), as a substrate (Fig. 5A; Fig. S1). During incubation with the active purified protease we did not detect any decrease in the level of FLAG-tagged PsaA (F.PsaA) and only a small decrease in PsaB (−EDTA) when compared with the negative control

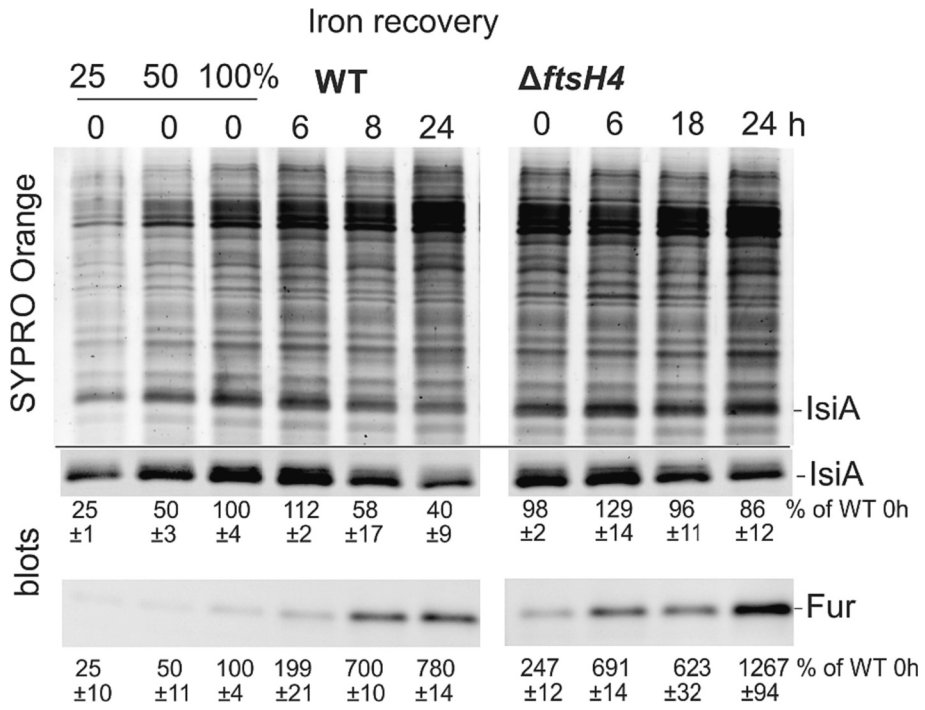

Fig. 4. Levels of IsiA in WT and Δ*ftsH4* cells after iron depletion and during the recovery from iron stress. Membrane proteins were isolated from WT and Δ*ftsH4* mutant exposed to iron depletion for 72 h and then were harvested at 0 h, 6 h, 18 h, and 24 h after the shift from iron depletion to normal BG11 medium (+Fe^{2+}). Membrane proteins were separated by SDS-PAGE and stained by SYPRO Orange, electroblotted to PVDF membrane and the blot probed with antibodies specific for IsiA and Fur. Samples were loaded per the same $OD_{750\ nm}$ of 0.3. The obtained protein signals were quantified by AzureSpot Pro software v. 2.2.107 (Azure Biosystems). A ratio (percentage) of each analysed substrate in comparison to 100 % in calibration is shown, values are means of 3 independent measurements ± standard deviation.

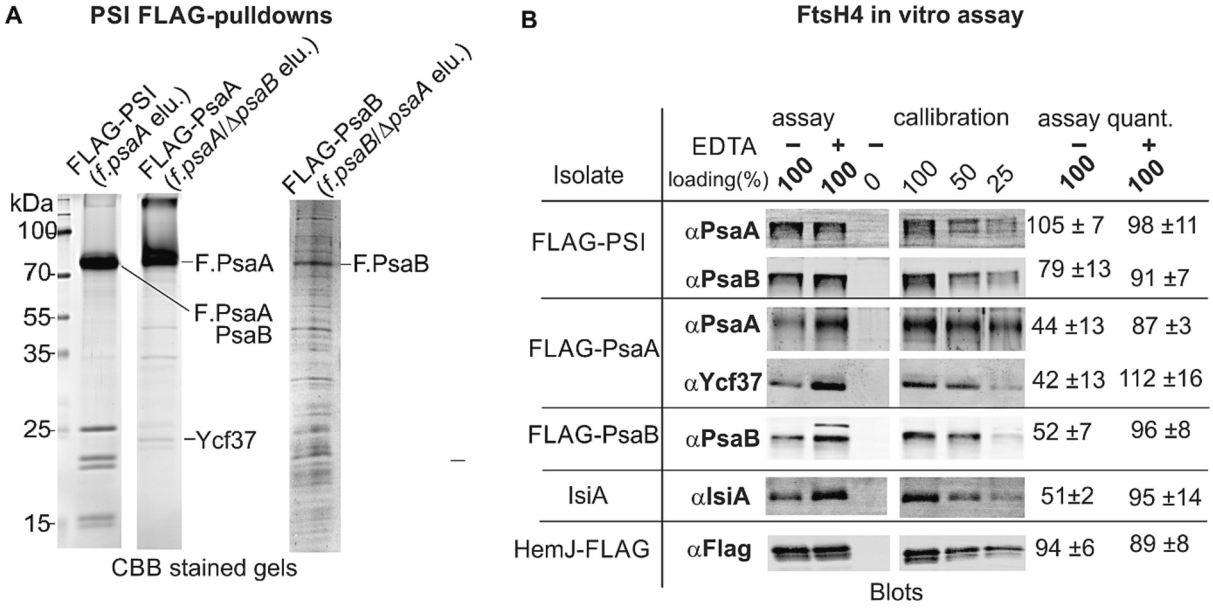

Fig. 5. Isolation of PSI, unassembled FLAG-PsaA/FLAG-PsaB subunits, IsiA and their digestion by FtsH4 *in vitro*. A) Analysis of PSI FLAG pulldowns. FLAG-PSI is an intact PSI complex isolated using F.PsaA protein produced in WT background (*f.psaA* strain) while the FLAG-PsaA (*f.psaA/ΔpsaB strain*) and FLAG-PsaB (*f.psaB/ΔpsaA strain*) elutions contained unassembled PSI core proteins. 10 µl of 10 times concentrated pulldowns were loaded onto the gel, which was then stained with Coomassie Blue. The identity of Ycf37 was verified by MS and immunodetection (Fig. S6B). B) FLAG-PSI, FLAG-PsaA, FLAG-PsaB and HemJ-FLAG pulldowns and IsiA gel extract were used as substrates for the FtsH4 activity assay. Adding 5 mM EDTA (+) inhibits the protease activity. At the start of the reaction, samples contained 0.3 µg of FtsH4 protein and 0.2 µg of the substrate in total, corresponding to 100 % in calibration; a control sample with no substrate added (0 %) is also shown. All samples were incubated for 3 h at 37 °C (see Material and Methods for details). After incubation, the samples were separated by SDS-PAGE, electroblotted to PVDF membrane and the presence of substrates and FtsH4 was detected by antibodies. According to substrate calibration, the obtained protein signals (in B) were quantified by AzureSpot Pro software v. 2.2.107 (Azure Biosystems). A ratio (percentage) of each analysed substrate in comparison to 100 % in calibration is shown, values are means of 3 independent reactions ± standard deviation. (For interpretation of the references to colour in this figure legend, the reader is referred to the web version of this article.)

(+EDTA) or with 100 % of a substrate in a calibration line (Fig. 5B). It indicates that the core proteins assembled in the PSI complex are not easily degraded by the FtsH4 protease.

To obtain unassembled PSI core subunits for the FtsH4 assay, we constructed *Synechocystis* strains producing either F.PsaA or FLAG-PsaB (F.PsaB) only, each in a genetic background lacking the second PSI core subunits (*f.psaA/ΔpsaB* and *f.psaB/ΔpsaA* strains — see Fig. S1). The resulting mutants showed a typical ΔPSI phenotype with a very low Chl level [48]. Importantly, F.PsaA and F.PsaB proteins could be detected by anti-FLAG antibody (Fig. S6A) and isolated, albeit the accumulation of FLAG-PsaB in TM is much lower than of FLAG-PsaA (Fig. S6A) and the amount of the purified F.PsaB is also low (Fig. 5A). Notably, the Ycf37 factor was co-eluted with F.PsaA (Fig. S6B) allowing us to test the Ycf37 as a substrate for FtsH4.

Fig. 5B shows that after 3 h in the assay, the amount of the Ycf37 decreased by >60 %. As expected, the substrate levels were not reduced in a control sample containing 5 mM EDTA. Importantly, by utilizing the unassembled F.PsaA and F.PsaB subunits as substrates, about half of this protein content was degraded.

To isolate IsiA as a substrate for *in vitro* FtsH4 assay, we separated membranes from WT grown under 72 h of iron depletion on the CN gel and extracted IsiA complexes from the CN gel. We focused on the monomeric IsiA not assembled with the PSI complex, (see Fig. S6C). The amount of IsiA decreased by 50 % after 3 h of the reaction with active FtsH4 protease while IsiA levels were only slightly reduced in a control sample containing 5 mM EDTA (Fig. 5B). These results also suggest that FtsH4 can degrade IsiA *in vitro*. We checked also the potential degradation of protoporphyrinogen IX oxidase enzyme (HemJ, Slr1790) involved in tetrapyrrole biosynthesis. This enzyme was identified among the 44 putative substrates of FtsH4 by MS and the purified FLAG-tagged HemJ protein (HemJ.f) is available in our laboratory [49]. However, we did not observe any significant decrease, which implies that this protein was not degraded by FtsH4 *in vitro*.

4. Discussion

The cyanobacterial FtsH4 and its plastid orthologs (*e.g. A. thaliana* AtFtsH7 and AtFtsH9) form a distinct phylogenetic subgroup of FtsH proteases [50]. These homo-oligomeric FtsHs differ structurally from hetero-oligomeric FtsH1/3 and FtsH2/3 and corresponding chloroplast FtsH2/FtsH8 complexes and seem to have little or no functional overlap with them. The unique function of FtsH4 is documented by a different regulation of this protease complex in *Synechocystis* (Fig. S3). While the level of FtsH1/2 and FtsH2/3 complexes decreased in the stationary phase and increased after shift to HL, the level of FtsH4 increased during the transition to stationary phase with its peak in linear growth phase and decreased after long-term exposition to HL. Different regulation was also observed at the transcript level (Fig. S2 [51]).

Recently, we have shown that the FtsH4 complex is not involved in the repair of PSII damaged by high irradiance or oxidative stress [7]. However, it is required for efficient acclimation of cell to sudden changes in light intensity. It controls the biogenesis of PSII by dual regulation of the level of Hlips [17]. Firstly, FtsH4 promotes the expression of Hlips after shift to high irradiance, most likely by modulation of the Hik33/RpaB regulon [7]. This role seems to be particularly crucial for cells exposed to HL after reaching the stationary phase; under these conditions the lack of FtsH4 is lethal. At another regulatory level, the FtsH4 controls the turnover of Hlips and degrades these proteins once stress conditions relieve [7].

In this work, we applied the substrate trapping approach to identify additional putative FtsH4 substrates. The identified candidates for substrate were predominantly membrane proteins related to photosynthesis (Table S2). We did not detect Hlips HliA, HliB, and HliC as (already known) substrates of FtsH4 [7], however, the cell cultures used for pulldowns were grown under conditions that do not induce a high expression of the *hliA-C* genes. The constitutively produced HliD protein [52] was 3.5-fold more abundant in our trap pulldown compared with the active FtsH4 form but did not meet our strict criteria for significance. Although the HliD is most likely the 'true' substrate of FtsH4, the detection of very small hydrophobic proteins by MS is problematic, especially when they are present in lower amounts. It is possible that other small membrane proteins were not detected as statistically significant substrate candidates due to the limits in their MS detectability.

On the other hand, the identification of Ycf4 and Ycf37 assembly factors as FtsH4 substrates looks quite convincing. In WT, the expression of *ycf4* and *ycf37* genes remains stable after shift of cells to HL [51], but the level of these proteins is significantly reduced (Fig. 3). We found lower content of Ycf37 in the F4CF mutant overexpressing FtsH4 in comparison with WT (Fig. 3B) but there was no HL-induced degradation of Ycf37 and Ycf4 in the FtsH4 deletion mutant (Fig. 3C). In addition, the digestion of Ycf37 by FtsH4 protease was confirmed *in vitro* (Fig. 5). Our results also suggest that FtsH4 can regulate the level of both PsaB and PsaA PSI core proteins. Nevertheless, *in vivo* and *in vitro* analyses suggest that the FtsH4 protease is involved in degradation of unassembled PsaA or PsaB core subunits rather than the intact PSI complex (Figs. 4 and 5). The *in vitro* digestion was however not so efficient as in the case of small proteins such are Hlips or Ycf37, which might be due to the large mass of PsaA/B (~ 80 kDa). Since the FtsH4 exhibits strong auto-proteolytic activity [7], the protease itself might be simply degraded faster than the large substrate. Notably, the level of PSI in FtsH4-less cells is aberrantly high [7] (Fig. S5) and this mutant also accumulates PSI assembly intermediates (Fig. 2) when exposed to cold stress. We therefore propose that the FtsH4 degrades the Ycf4 and Ycf37 factors under conditions when the PSI biogenesis needs to be rapidly arrested; typically, after shifting *Synechocystis* cells from NL to HL. As shown previously in [53], in the first hours at HL, *Synechocystis* strongly reduces the synthesis of PSI to 'dilute' the cellular concentration of this complex, thereby adjusting the PSI to PSII stoichiometry for HL. This new ratio is then stabilized in HL-acclimated cells [53].

Both Ycf37 and Ycf4 are involved in the early steps of PSI assembly [26,54] and we therefore speculate that the FtsH4 limits the biogenesis of new PSI by lowering the level of assembly factors. The remaining free PSI core subunits and partially assembled PSI complexes can also be degraded by FtsH4 (Fig. 5). Because Chl biosynthesis is almost completely blocked for 2–3 h after shift to HL (Sobotka, R, unpublished data), Chl molecules, released from PSI assembly complexes, might be important for the maintenance of active PSII complexes during the early stage of acclimation to HL. This hypothesis is in line with the patchy localization of FtsH4 at the periphery of TM where the biogenesis of photosynthetic apparatus is expected to occur [7,54]. The current study confirmed that the FtsH4 co-localizes with YidC and rubredoxin A proteins involved in the biosynthesis and assembly of photosystem proteins [19,37] (Supplementary Dataset 1). As it is speculated that the PSII and PSI biogenesis proceeds in a coordinated way [54], it is likely that FtsH4 modulates the biogenesis of both photosystems.

Another PSI-related protein identified as a putative substrate of FtsH4 is IsiA. This protein is homologous to PSII core antenna protein CP43 and it is massively produced in cyanobacteria under iron deficiency — it can bind up to 50 % of Chl in iron-starved cyanobacteria [55]. During the recovery from iron limitation, this large Chl deposit is probably released from degraded IsiA to support building of new photosystems [55]. The expression of the *isiA* gene is also induced, but to a lesser extent, under oxidative or HL stress and in the stationary phase, while it is subdued under optimal conditions. We did not observe any accumulation of IsiA in membranes isolated from *ftsH4-his* and ^{trap}*ftsH4-his* cells (Fig. S4), the level of this protein was apparently very low and the interaction between IsiA and FtsH4 thus must be very specific. The control of IsiA level by FtsH4 is supported by delayed IsiA degradation in Δ*ftsH4* mutant during the recovery from iron depletion (Fig. 4). It should be noted that IsiA was still degraded in Δ*ftsH4* (Fig. 4) and it is thus quite likely that other proteases participate in the IsiA digestion.

Although we focused on validation of substrates that are related to

the PSI complex, it is worth mentioning other proteins identified by our FtsH4 trap assay. One of the most prominent hits was the PetD subunit of the cytochrome b_6f complex. PetD binds the Chl molecule in cytochrome b_6f [56] and therefore exhibits the highest probability of the oxidative damage induced by this excited Chl. In line with its higher turnover, PetD is the only subunit of the complex which shows a clear radioactive labelling in *Synechocystis* (Fig. S6). Notably, components of cytochrome b_6f have already been considered a potential FtsH substrate in *Chlamydomonas* [6].

Remarkable is also the enrichment of proteins connected with CO_2 concentrating mechanism such as SbtA, SbtB, and CupA. Since their accumulation together with flavoproteins, Slr1634, Ycf23, and Sll1514 increases in response to low CO_2 and is controlled by NdhR regulon [57], we do not assume that all these hits are FtsH4 substrates. In fact, the level of these proteins might be just high in ^{trap}*ftsH4-his* strain due to the lack of FtsH4 (regulatory) activity. Alternatively, some of these proteins are real substrates but others are pulled out due to interaction with the substrate. For instance, SbtB, Flv2, and Flv4 were present only in the trap pulldown while other CCM proteins were co-isolated with active protease. Hypothetically, SbtB or Flv2/4 specifically trapped in inactive FtsH4 might serve as FtsH4 substrates associated with other proteins. These results, together with the fact that the FtsH4-His is copurified with Slr0374, another protein important for CO_2 uptake, suggest that the FtsH4 plays an important role in the acquisition of inorganic carbon.

Supplementary data to this article can be found online at https://doi.org/10.1016/j.bbabio.2023.149017.

CRediT authorship contribution statement

V.K., R.S., J.K. and P.K. designed the study, P.K., V.K., M.T., P.S. and S.D. performed research and obtained all results; V.K., R.S., J.K. and P.K. analysed data and wrote the paper. All authors discussed and critically read the manuscript.

Declaration of competing interest

The authors declare that they have no known competing financial interests or personal relationships that could have appeared to influence the work reported in this paper.

Data availability

The MS proteomics data were deposited in the MassIVE. The link to the MS Data will be shared in Manuscript in Method section

Acknowledgements

This work was supported by the Czech Science Foundation (19-08900Y to V.K., 19-29225X to J.K. and R.S.). P.K. acknowledges support from the Czech Ministry of Education, Youth and Sport (CZ.02.1.01/0.0/0.0/15_003/0000441).

References

[1] K. Ito, Y. Akiyama, Cellular functions, mechanism of action, and regulation of FtsH protease, Annu. Rev. Microbiol. 59 (2005) 211–231.
[2] Z. Adam, A. Zaltsman, G. Sinvany-Villalobo, W. Sakamoto, FtsH proteases in chloroplasts and cyanobacteria, Physiol. Plant. 123 (2005) 386–390.
[3] S. Jarvi, M. Suorsa, L. Tadini, A. Ivanauskaite, S. Rantala, Y. Allahverdiyeva, D. Leister, E.M. Aro, Thylakoid-bound FtsH proteins facilitate proper biosynthesis of photosystem I, Plant Physiol. 171 (2016) 1333–1343.
[4] Y. Kato, E. Miura, R. Matsushima, W. Sakamoto, White leaf sectors in yellow variegated2 are formed by viable cells with undifferentiated plastids, Plant Physiol. 144 (2007) 952–960.
[5] M. Yoshioka, S. Uchida, H. Mori, K. Komayama, S. Ohira, N. Morita, T. Nakanishi, Y. Yamamoto, Quality control of photosystem II — cleavage of reaction center D1 protein in spinach thylakoids by FtsH protease under moderate heat stress, J. Biol. Chem. 281 (2006) 21660–21669.
[6] A. Malnoe, F. Wang, J. Girard-Bascou, F.-A. Wollman, C. de Vitry, Thylakoid FtsH protease contributes to photosystem II and cytochrome b_6f remodeling in *Chlamydomonas reinhardtii* under stress conditions, Plant Cell 26 (2014) 373–390.
[7] V. Krynická, P. Skotnicová, P.J. Jackson, S. Barnett, J. Yu, A. Wysocka, R. Kaňa, M. J. Dickman, P.J. Nixon, C.N. Hunter, J. Komenda, FtsH4 protease controls biogenesis of the PSII complex by dual regulation of high light-inducible proteins, Plant Commun. 4 (2023), 100502.
[8] P.J. Jackson, A. Hitchcock, A.A. Brindley, M.J. Dickman, C.N. Hunter, Absolute quantification of cellular levels of photosynthesis-related proteins in *Synechocystis* sp. PCC 6803, Photosynth. Res. 155 (2023) 219–245.
[9] F. Yu, S. Park, S.R. Rodermel, The *Arabidopsis* FtsH metalloprotease gene family: interchangeability of subunits in chloroplast oligomeric complexes, Plant J. 37 (2004) 864–876.
[10] P. Silva, E. Thompson, S. Bailey, O. Kruse, C.W. Mullineaux, C. Robinson, N. H. Mann, P.J. Nixon, FtsH is involved in the early stages of repair of photosystem II in *Synechocystis* sp PCC 6803, Plant Cell 15 (2003) 2152–2164.
[11] V. Krynická, S. Shao, P.J. Nixon, J. Komenda, Accessibility controls selective degradation of photosystem II subunits by FtsH protease, Nat. Plants 1 (2015).
[12] J. Komenda, M. Barker, S. Kuviková, R. de Vries, C.W. Mullineaux, M. Tichý, P. J. Nixon, The FtsH protease *slr0228* is important for quality control of photosystem II in the thylakoid membrane of *Synechocystis* sp PCC 6803, J. Biol. Chem. 281 (2006) 1145–1151.
[13] N.H. Mann, N. Novac, C.W. Mullineaux, J. Newman, S. Bailey, C. Robinson, Involvement of an FtsH homologue in the assembly of functional photosystem I in the cyanobacterium *Synechocystis* sp PCC 6803, FEBS Lett. 479 (2000) 72–77.
[14] J. Sacharz, S.J. Bryan, J. Yu, N.J. Burroughs, E.M. Spence, P.J. Nixon, C. W. Mullineaux, Sub-cellular location of FtsH proteases in the cyanobacterium *Synechocystis* sp PCC 6803 suggests localised PSII repair zones in the thylakoid membranes, Mol. Microbiol. 96 (2015) 448–462.
[15] V. Krynická, M. Tichý, J. Krafl, J. Yu, R. Kana, M. Boehm, P.J. Nixon, J. Komenda, Two essential FtsH proteases control the level of the Fur repressor during iron deficiency in the cyanobacterium *Synechocystis* sp PCC 6803, Mol. Microbiol. 94 (2014) 609–624.
[16] V. Krynická, J. Georg, P.J. Jackson, M.J. Dickman, C.N. Hunter, M.E. Futschik, W. R. Hess, J. Komenda, Depletion of the FtsH1/3 proteolytic complex suppresses the nutrient stress response in the cyanobacterium *Synechocystis* sp strain PCC 6803, Plant Cell 31 (2019) 2912–2928.
[17] J. Komenda, R. Sobotka, Cyanobacterial high-light-inducible proteins—protectors of chlorophyll-protein synthesis and assembly, Biochim. Biophys. Acta 1857 (2016) 288–295.
[18] M.M. Konert, A. Wysocka, P. Koník, R. Sobotka, High-light-inducible proteins HliA and HliB: pigment binding and protein-protein interactions, Photosynth. Res. 152 (2022) 317–332.
[19] J. Knoppová, R. Sobotka, J. Yu, M. Bečková, J. Pilný, J.P. Trinugroho, L. Csefalvay, D. Bína, P.J. Nixon, J. Komenda, Assembly of D1/D2 complexes of photosystem II: binding of pigments and a network of auxiliary proteins, Plant Physiol. 187 (2022) 790–804.
[20] M. Tichý, B. Martina, J. Kopečná, J. Noda, R. Sobotka, J. Komenda, Strain of *Synechocystis* PCC 6803 with aberrant assembly of photosystem II contains tandem duplication of a large chromosomal region, Front. Plant Sci. 7 (2016).
[21] J.G. Metz, P.J. Nixon, M. Rögner, G.W. Brudvig, B.A. Diner, Directed alteration of the D1 polypeptide of photosystem II: evidence that tyrosine-161 is the redox component, Z, connecting the oxygen-evolving complex to the primary electron donor, P680, Biochemistry 28 (1989) 6960–6969.
[22] R.J. Porra, W.A. Thompson, P.E. Kriedemann, Determination of accurate extinction coefficients and simultaneous equations for assaying chlorophylls a and b extracted with four different solvents: verification of the concentration of chlorophyll standards by atomic absorption spectroscopy, Biochim. Biophys. Acta Bioenerg. 975 (1989) 384–394.
[23] J. Komenda, V. Krynická, T. Zakar, Isolation of thylakoid membranes from the cyanobacterium *Synechocystis* sp. PCC 6803 and analysis of their photosynthetic pigment-protein complexes by Clear Native-PAGE, Bio Protoc. 9 (2019).
[24] M. Boehm, J. Yu, V. Krynická, M. Barker, M. Tichý, J. Komenda, P.J. Nixon, J. Nield, Subunit organization of a *Synechocystis* hetero-oligomeric thylakoid FtsH complex involved in photosystem II repair, Plant Cell 24 (2012) 3669–3683.
[25] Q. Xu, Y.S. Jung, V.P. Chitnis, J.A. Guikema, J.H. Golbeck, P.R. Chitnis, Mutational analysis of photosystem I polypeptides in *Synechocystis* sp. PCC 6803. Subunit requirements for reduction of NADP+ mediated by ferredoxin and flavodoxin, J. Biol. Chem. 269 (1994) 21512–21518.
[26] U. Dühring, K.D. Irrgang, K. Lünser, J. Kehr, A. Wilde, Analysis of photosynthetic complexes from a cyanobacterial ycf37 mutant, Biochim. Biophys. Acta 1757 (2006) 3–11.
[27] M. Koskela, P. Skotnicová, E. Kiss, R. Sobotka, Purification of protein-complexes from the cyanobacterium *Synechocystis* sp. PCC 6803 using FLAG-affinity chromatography, Bio Protoc. 10 (2020).
[28] T. Tomoyasu, J. Gamer, B. Bukau, M. Kanemori, H. Mori, A.J. Rutman, A. B. Oppenheim, T. Yura, K. Yamanaka, H. Niki, S. Hiraga, T. Ogura, *Escherichia coli* FtsH is a membrane-bound, ATP-dependent protease which degrades the heat-shock transcription factor sigma 32, EMBO J. 14 (1995) 2551–2560.
[29] J. Rappsilber, M. Mann, Y. Ishihama, Protocol for micro-purification, enrichment, pre-fractionation and storage of peptides for proteomics using StageTips, Nat. Protoc. 2 (2007) 1896–1906.
[30] J. Cox, M. Mann, MaxQuant enables high peptide identification rates, individualized p.p.b.-range mass accuracies and proteome-wide protein quantification, Nat. Biotechnol. 26 (2008) 1367–1372.

[31] S. Tyanova, T. Temu, J. Cox, The MaxQuant computational platform for mass 0spectrometry-based shotgun proteomics, Nat. Protoc. 11 (2016) 2301–2319.
[32] S. Tyanova, T. Temu, P. Sinitcyn, A. Carlson, M.Y. Hein, T. Geiger, M. Mann, J. Cox, The Perseus computational platform for comprehensive analysis of (prote) omics data, Nat. Methods 13 (2016) 731–740.
[33] L. Atorino, L. Silvestri, M. Koppen, L. Cassina, A. Ballabio, R. Marconi, T. Langer, G. Casari, Loss of m-AAA protease in mitochondria causes complex I deficiency and increased sensitivity to oxidative stress in hereditary spastic paraplegia, J. Cell Biol. 163 (2003) 777–787.
[34] K. Westphal, S. Langklotz, N. Thomanek, F. Narberhaus, A trapping approach reveals novel substrates and physiological functions of the essential protease FtsH in *Escherichia coli*, J. Biol. Chem. 287 (2012) 42962–42971.
[35] B. Schwanhausser, D. Busse, N. Li, G. Dittmar, J. Schuchhardt, J. Wolf, W. Chen, M. Selbach, Global quantification of mammalian gene expression control, Nature 473 (2011) 337–342.
[36] H.B. Jiang, W.Y. Song, H.M. Cheng, B.S. Qiu, The hypothetical protein Ycf46 is involved in regulation of CO_2 utilization in the cyanobacterium *Synechocystis* sp. PCC 6803, Planta 241 (2015) 145–155.
[37] É. Kiss, J. Knoppová, G.P. Aznar, J. Pilný, J. Yu, P. Halada, P.J. Nixon, R. Sobotka, J. Komenda, A photosynthesis-specific Rubredoxin-like protein is required for efficient association of the D1 and D2 proteins during the initial steps of photosystem II assembly, Plant Cell 31 (2019) 2241–2258.
[38] E.J. Boekema, A. Hifney, A.E. Yakushevska, M. Piotrowski, W. Keegstra, S. Berry, K.P. Michel, E.K. Pistorius, J. Kruip, A giant chlorophyll-protein complex induced by iron deficiency in cyanobacteria, Nature 412 (2001) 745–748.
[39] T.S. Bibby, J. Nield, J. Barber, Iron deficiency induces the formation of an antenna ring around trimeric photosystem I in cyanobacteria, Nature 412 (2001) 743–745.
[40] C.E. Lubner, R. Grimme, D.A. Bryant, J.H. Golbeck, Wiring photosystem I for direct solar hydrogen production, Biochemistry 49 (2010) 404–414.
[41] J.H. Golbeck, D.A. Bryant, Photosystem I, in: C.P. Lee (Ed.), Current Topics in Bioenergetics, Academic Press, 1991, pp. 83–177.
[42] J.-D. Rochaix, Chloroplast reverse genetics: new insights into the function of plastid genes, Trends Plant Sci. 2 (1997) 419–425.
[43] A. Wilde, K. Lünser, F. Ossenbühl, J. Nickelsen, T. Börner, Characterization of the cyanobacterial ycf37: mutation decreases the photosystem I content, Biochem. J. 357 (2001) 211–216.
[44] I. Orf, D. Schwarz, A. Kaplan, J. Kopka, W.R. Hess, M. Hagemann, S. Klähn, CyAbrB2 contributes to the transcriptional regulation of low CO_2 acclimation in *Synechocystis* sp. PCC 6803, Plant Cell. Physiol. 57 (2016) 2232–2243.
[45] Y. Hihara, K. Sonoike, Regulation, inhibition and protection of photosystem I, in: E.-M. Aro, B. Andersson (Eds.), Regulation of Photosynthesis, Springer, Netherlands, Dordrecht, 2001, pp. 507–531.
[46] Regulation of Photosynthesis, 1st ed., Springer Netherlands, 2001. Imprint: Springer, Dordrecht, 2001.
[47] A.K. Singh, L.A. Sherman, Iron-independent dynamics of IsiA production during the transition to stationary phase in the cyanobacterium *Synechocystis* sp PCC 6803, FEMS Microbiol. Lett. 256 (2006) 159–164.
[48] G. Shen, W.F. Vermaas, Chlorophyll in a *Synechocystis* sp. PCC 6803 mutant without photosystem I and photosystem II core complexes. Evidence for peripheral antenna chlorophylls in cyanobacteria, J. Biol. Chem. 269 (1994) 13904–13910.
[49] P. Skotnicová, R. Sobotka, M. Shepherd, J. Hájek, P. Hrouzek, M. Tichý, The cyanobacterial protoporphyrinogen oxidase HemJ is a new b-type heme protein functionally coupled with coproporphyrinogen III oxidase, J. Biol. Chem. 293 (2018) 12394–12404.
[50] T. Cardona, S. Shao, P.J. Nixon, Early emergence of the FtsH proteases involved in photosystem II repair, Photosynthetica 56 (2018) 163–177.
[51] M. Kopf, S. Klaehn, I. Scholz, J.K.F. Matthiessen, W.R. Hess, B. Voss, Comparative analysis of the primary transcriptome of *Synechocystis* sp PCC 6803, DNA Res. 21 (2014) 527–539.
[52] Q. He, N. Dolganov, O. Bjorkman, A.R. Grossman, The high light-inducible polypeptides in *Synechocystis* PCC6803. Expression and function in high light, J. Biol. Chem. 276 (2001) 306–314.
[53] J. Kopečná, J. Komenda, L. Bučinská, R. Sobotka, Long-term acclimation of the cyanobacterium *Synechocystis* sp PCC 6803 to high light is accompanied by an enhanced production of chlorophyll that is preferentially channeled to trimeric photosystem I, Plant Physiol. 160 (2012) 2239–2250.
[54] J. Komenda, R. Sobotka, Chlorophyll-binding subunits of photosystem I and II: biosynthesis, chlorophyll incorporation and assembly, Adv. Bot. Res. 91 (2019) 195–223.
[55] A. Jia, Y. Zheng, H. Chen, Q. Wang, Regulation and functional complexity of the chlorophyll-binding protein IsiA, Front. Microbiol. 12 (2021), 774107.
[56] W.A. Cramer, Structure-function of the cytochrome b(6)f lipoprotein complex: a scientific odyssey and personal perspective, Photosynth. Res. 139 (2019) 53–65.
[57] S. Klähn, I. Orf, D. Schwarz, J.K.F. Matthiessen, J. Kopka, W.R. Hess, M. Hagemann, Integrated transcriptomic and metabolomic characterization of the low-carbon response using an ndhR mutant of *Synechocystis* sp PCC 6803, Plant Physiol. 169 (2015) 1540–1556.